

# ION BEAM DYNAMICS IN THE ACCELERATION REGION OF THE VINČY CYCLOTRON

S. S. TOMIĆ, N. NEŠKOVIĆ, P. BELIČEV

Laboratory of Physics (010), Vinča Institute of Nuclear Sciences, P. O. Box 522, 11000 Belgrade, Yugoslavia

E. V. SAMSONOV

Laboratory of Nuclear Problems, Joint Institute for Nuclear Research, 141980 Dubna, Moscow region, Russia

The modern concept of heavy ion cyclotrons assumes the tendency of decreasing the gaps between poles of the magnet, enabling a better efficiency of the magnetic circuit. This assumption restricts the possible solutions of accelerating structure, and imposes the necessity of placing the dees in valleys of the magnet. This approach, which is accepted for the VINČY Cyclotron, the main part of the TESLA Accelerator Installation, requires a detailed study of the ion beam dynamics in the acceleration region. Consequently, we analyze the behaviour of the ion beams with specific charge equal to 1, 0.5 and 0.25 in the radial and axial phase spaces. Also, the energy spread within the emittances and the influence of the first harmonic of the magnetic field on the radial betatron oscillations are discussed.

## 1 Introduction

VINČY Cyclotron [1] is a multiparticle and multipurpose machine which is under construction in the Vinča Institute of Nuclear Sciences, Belgrade, Yugoslavia. To illustrate its design some main parameters are listed in table 1.

Table 1 : Main parameters of the VINČY Cyclotron.

Type of accelerated part.	$\eta = Z/A$	0.15-1.0
Bending limit	[MeV]	145
Focusing limit	[MeV]	75
Magnetic pole diameter	[cm]	200
Number of sectors		4
Spirality of sectors	[°]	0
Angular span of sectors	[°]	42
Hill gap	[cm]	3.1
Valley gap	[cm]	19
Number of trim coils		10
Number of harmonic coils		8
Number of dees		2
Angular span of dees	[°]	40
Frequency range	[MHz]	17-31
Harmonic numbers	$h = \omega_{RF}/\omega$	1-4
Vertical aperture of dees	[cm]	2.2
Maximal dee voltage	[kV]	100

In order to be sure in the validity of chosen parameters of magnetic field, a series of dynamical calculations in the main acceleration region have been done. During these computations we paid attention to accurate estimations of transverse oscillation amplitudes, betatron frequencies, phase motion and parameters of some beams in the extraction region of the Cyclotron. Influence of the first harmonic of the magnetic field the imperfections

on beam parameters along main acceleration region was also studied. As a result we obtained a probable range of the parameters of the beams on the stripping foil located in the extraction region. In order to evaluate permissible degree of dee misalignments some computations were fulfilled for shifted and twisted dees. Obtained results showed a rather strict tolerance to dee position.

## 2 Ion beam dynamics

Three types of particles have been used in the dynamic computation:  $H^-$ ,  $D^-$  and  $^{20}Ne^{5+}$ . Emittances of these beams on the beginning of acceleration were obtained earlier [2] after extensive work concerning optimization of the central region geometry. Initial parameters of the beams are represented in table 2.

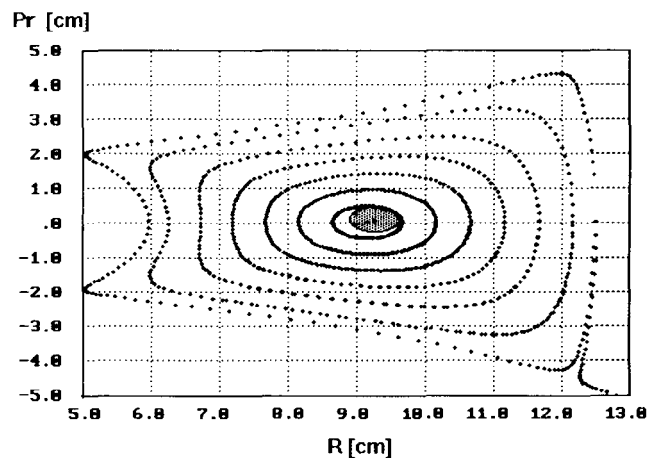


Figure 1: Relative position of AEO with respect to the static phase plot for  $H^-$  ions.

All beams were accelerated starting from the accelerated equilibrium orbits (AEO) [3], in order to minimize the amplitude of radial betatron oscillations below 1 mm. Position of AEO relative to the static phase plot in radial phase space for particles with specific charge  $\eta = 1$  are shown on figure 1. Increasing the distance from the stable fixed point representing the static equilibrium orbit (SEO), the ellipse-like contours degenerate into geometrical forms of 4-fold symmetry, where 4 is the order of the driving perturbation force induced by the dominant resonance  $Q_r = N/4$ , and  $N = 4$  is the magnetic field periodicity. The separatrix distance is  $R = 3.25$  cm from AEO.

Between 100 and 1000 particles were generated randomly by correlated Gauss distribution inside 6D phase volume around AEO. Then, these particles have been accelerated for 500, 260 and 112 turns in the case of  $H^-$ ,  $D^-$  and  $^{20}\text{Ne}^{5+}$ , respectively. The dee gap electric field is given by [4]:

$$E_y = \frac{U_{\text{RF}}}{\Delta y \sqrt{2\pi}} \exp \left[ -\frac{1}{2} \left( \frac{y}{\Delta y} \right)^2 \right] \cos[h(\omega t - \psi_0)] \quad (1)$$

$$E_z = \frac{yzE_y}{\Delta y^2} \left\{ 1 + \frac{1}{6} \left( \frac{z}{\Delta y} \right)^2 \left[ \left( \frac{y}{\Delta y} \right)^2 - 3 \right] + \dots \right\} \quad (2)$$

where  $\Delta y = 0.2H + 0.4W$ ,  $E_y$  and  $E_z$  are the horizontal and vertical components of the electric field,  $U_{\text{RF}}$  is the dee voltage,  $H$  is the axial aperture of the dee,  $W$  is the areacceleration gap width,  $\omega$  is the frequency of particle rotation, and  $\psi_0$  is the initial particle phase relative to the RF system.

Table 2 : Initial parameters of the beams.

Type of particles		$H^-$	$D^-$	$^{20}\text{Ne}^{5+}$
Energy	[MeV/n]	0.726	0.300	0.080
Radius of central particle	[cm]	9.260	8.518	8.270
Emittances:				
radial (normalized)	[ $\pi$ mm mrad]	2.08	1.72	2.43
radial (unnormalized)	[ $\pi$ mm mrad]	52.9	68.1	185.8
axial (unnormalized)	[ $\pi$ mm mrad]	13.8	21.8	13.8
Elongation from AEO:				
radial	[mm]	2.2	2.5	4.0
axial	[mm]	3.0	3.0	3.0
Dee voltage	[kV]	100	100	80
Revolution frequency	[MHz]	20.740	14.770	7.589
Harmonic number	$h$	1	2	4
Bunch phase width	$h \times [^\circ]$	15	40	40

Shape of magnetic pole sectors of the Cyclotron was chosen after a series of 2D and 3D calculations [5] as well as on the bases of experimental results obtained using a magnet model (scale 1:10) [6]. Smoothed experimental data describing amplitude of main (fourth) harmonic of magnetic field for three levels of magnet excitation are shown in figure 2. These levels refer to three acceleration regimes which are considered. Also, in figure 2 the corresponding isochronous field which was obtained by the iteration procedure are presented [7].

Phase motion of bunch central particle is illustrated in figure 3 and betatron frequencies in figure 4. These results were obtained by means of integration of the equa-

tions of motion describing the longitudinal and transverse particle motion. One sees a small phase slip during the acceleration (less than  $10^\circ$  relative to RF). Betatron frequencies are far from dangerous resonances  $3Q_r = 4$  and  $Q_r = 2Q_z$ .

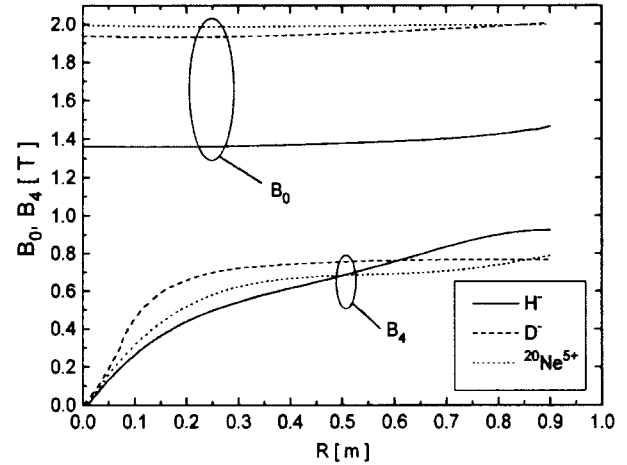


Figure 2: Isochronous and fourth harmonic fields for three types of particles.

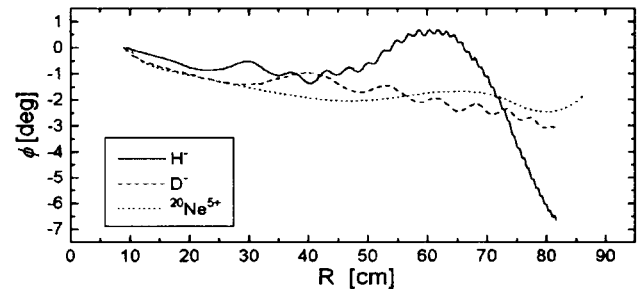


Figure 3: Phase motion of central particle of the bunch for  $\eta = 1$ , 0.5 and 0.25 ions.

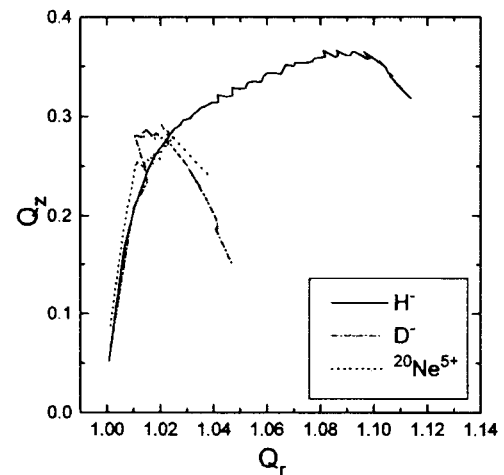


Figure 4: Central particle motion in the diagram of resonances for  $\eta = 1$ , 0.5 and 0.25 ions.

### 3 Beam current radial distribution

In order to check the quality of the beam radial motion we used a method of numerical differential probe. This probe, having the radial thickness of 1 mm, was moved along radius at azimuthal angle of probe PR1 (axis of symmetry of sector 1). Figure 5 shows the radial distribution of the current which was obtained in magnetic field without imperfections and after introducing the first harmonic of the magnetic field  $B_1 = 5 \times 10^{-4}$  T.

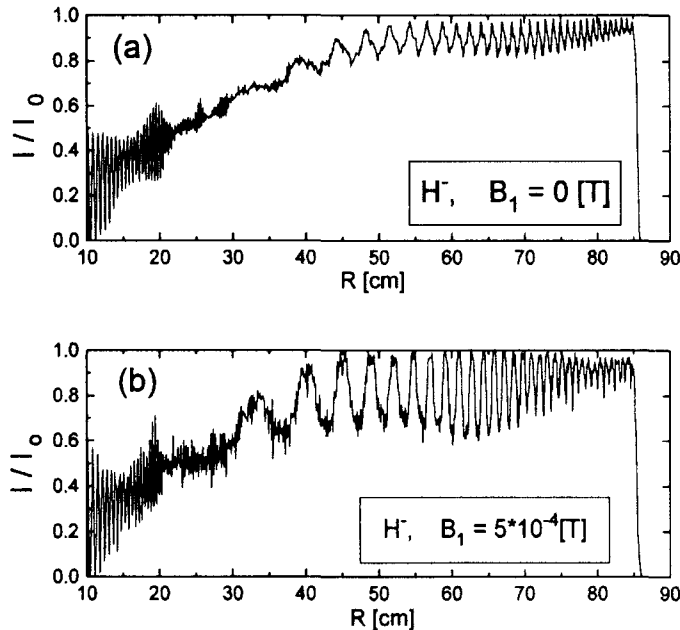


Figure 5: Current distribution obtained by 1 mm differential probe: without the first harmonic of the magnetic field (a), and with  $B_1=5 \times 10^{-4}$  T (b).

At the beginning of calculations central particle of the bunch had radial amplitude not large than 1 mm. In spite of this rather small amplitude, pulsations of current distribution are clearly visible at radii larger than 40 cm. The first harmonic of the field leads to the increase of coherent amplitude up to  $\sim 5$  mm and, as a result, pulsation of current becomes more distinct. Therefore, differential probe data should be considered as sensitive tool for estimation of beam centering in our machine.

### 4 Beam parameters on stripping foil

The light ions such as  $H^-$  and  $D^-$  will be extracted from the Cyclotron by the foil stripping system. This system is placed in the ranges of radius  $R \in [70, 86]$  cm and azimuthal angle  $\theta \in [225^\circ, 260^\circ]$ . In the calculations the stripping foils were located at  $R_{foil} = 79$  cm and  $\theta_{foil} = 249^\circ$  for  $H^-$ , and at  $R_{foil} = 78$  cm and  $\theta_{foil} = 252^\circ$  for  $D^-$  ions. In figure 6 we give the radial phase space for

the  $H^-$  beam that hits the foil. Normalized emittances

$$\epsilon_N = \gamma\beta\epsilon, \quad (3)$$

where  $\gamma = E/E_0$ ,  $\beta = v/c$  and  $\epsilon$  is unnormalized emittance, of the beam on the stripping foil are  $1.02\pi$  mm mrad and  $1.24\pi$  mm mrad for  $H^-$  and  $D^-$  ions, respectively, i.e. that is approximately 2.0 and 1.5 times smaller than initial values, respectively. This decrease is explained by the fact that radial size of the beam on stripping foil is smaller than initial one.

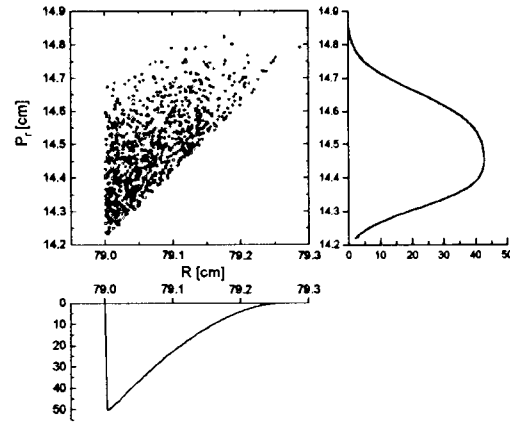


Figure 6: Radial phase space of  $H^-$  ions on stripping foil. Energy of particles in the beam is 60.8 MeV/n and energy spread within emittance is 0.7 %.

Computations showed that influence of first harmonic leads to increase of radial emittance,  $\epsilon_r$ , and energy spread of extracted beam,  $\Delta W/W$ . But this influence in the cases of  $H^-$  and  $D^-$  is rather different. It causes an essential increase of the radial emittance and small change of the energy spread for  $H^-$ . For  $D^-$  the picture is opposite. In any case one should conclude that  $B_1 = 5 \times 10^{-4}$  T leads to essential deterioration of beam parameters on the stripping foil. These results are presented in table 3.

Table 3 : Beam parameters on stripping foil.

Type of accelerated particles			$H^-$	$D^-$
W [MeV/n]			60.8	28.7
$B_1 = 0 [T]$	$\epsilon_r$	[ $\pi$ mm mrad]	2.76	4.93
	$\epsilon_{rN}$	[ $\pi$ mm mrad]	1.02	1.24
	$\Delta W/W$	[%]	0.7	1.4
$B_1 = 5 \times 10^{-4} [T]$	$\epsilon_r$	[ $\pi$ mm mrad]	7.00	5.54
	$\epsilon_{rN}$	[ $\pi$ mm mrad]	2.59	1.39
	$\Delta W/W$	[%]	0.83	2.6

### 5 Impact of dee misalignments on axial motion

Two types of dee misalignment have been considered:

- shift, when dees are moved as a whole in the vertical direction;

- twist, when dees are rotated by a small angle around their longitudinal axes.

In the case of shift the vertical displacement of dee edge relatively to anti-dee had a constant value along both acceleration gaps. In the case of twist the displacements had the opposite signs in two gaps and were proportional to the radius. Distortion of accelerating gaps causes the appearance of an additional axial electric field. In the process of acceleration the perturbation field behaves in different ways: it has the same sign inside the gaps for twisted dee, and the opposite signs for shifted dee. In figure 7 the first 20 turns of the axial motion of the  $H^-$  beam is shown, without and with dee misalignments. One can see that shift of dee causes the pulsation of axial beam size, while twist of dee leads to coherent oscillations.

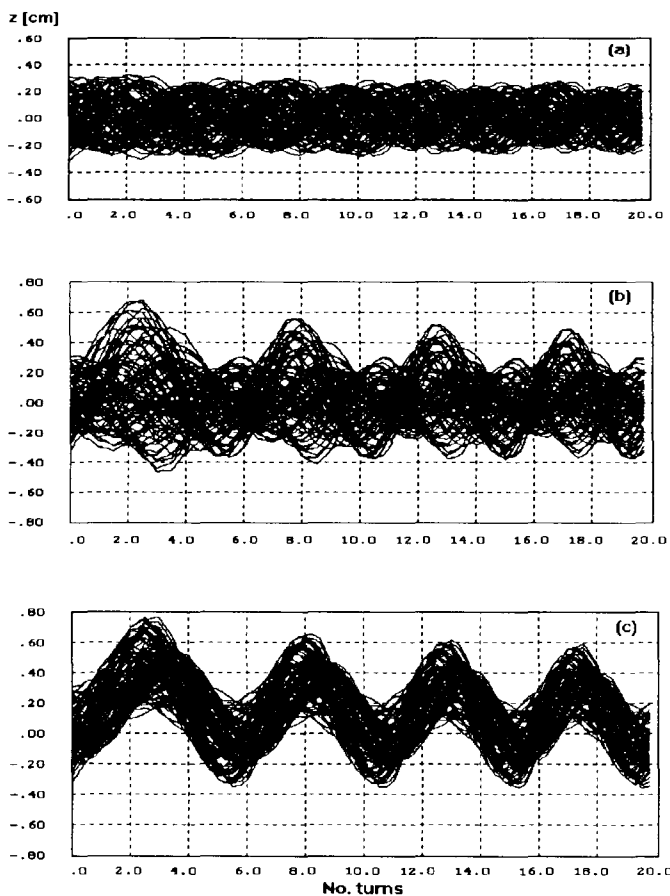


Figure 7: Axial motion of the beam without dee misalignments (a), dees are shifted by +2 mm (b), and dees are twisted by  $2^\circ$  (c).

Calculations showed that for radii larger than 10 cm shift of 0.5 mm and twist of  $0.5^\circ$  of the dees should be allowed without essential increase of beam size. The dee shift of 3 mm in  $z$  direction causes increase of axial beam envelope from 2.5 to 8 mm. This upper limit can be dangerous in Wallkinshaw resonance when beams are not correctly centered on AEO in the beginning of accelera-

tion process.

## 6 Conclusion

Adopted representation of acceleration field seems to be suitable in such type of calculations. Simulations showed stable particle motion in the acceleration region. Method of differential probe should be used in our machine to estimate radial coherent oscillations. First harmonic of magnetic field of  $5 \times 10^{-4}$  T causes essential deterioration of the beam quality on stripping foil. Dee position tolerances were evaluated concerning the beam axial motion. Beam dynamics in the VINCY Cyclotron shows excellent stability in the case of a good choice of starting conditions defined by central region shape.

## References

- [1] N. Nešković et al., "Status report on the VINCY Cyclotron", Proceedings of the 14th International Conference on Cyclotrons and their Applications, Cape Town, South Africa, pp. 82-85, 1995.
- [2] D. V. Altiparmakov, "Electrodes in the central region of the VINCY Cyclotron", Proceedings of the 12th Information meeting on the TESLA Accelerator Installation, Belgrade, Yugoslavia, 1997.
- [3] Lj. Milinković, K. Subotić and E. Fabrici, "Properties of centered accelerated equilibrium orbits", Nuc. Instr. and Meth., vol. A273, pp. 87-96, 1988.
- [4] N. Hazewindus, J. M. van Niewland, J. Faber and L. Leistra, "The magnetic analogue as used in the study of a cyclotron central region", Nuc. Instr. and Meth., vol. 118, pp. 125-134, 1974.
- [5] D. V. Altiparmakov, S. S. Tomić, M. V. Marković and N. A. Morozov, "Computer modeling of the isochronous field in the VINCY Cyclotron", Proceedings of the 14th International Conference on Cyclotrons and their Applications, Cape Town, South Africa, pp. 201-203, 1995.; D. V. Altiparmakov et al., "Operating range of the VINCY Cyclotron", Proceedings of the 5th EPAC, Barcelona, vol. 3, pp. 2210-2212, 1996.
- [6] S. Čirković et al., "Simulation of the VINCY Cyclotron magnetic field using a model magnet", Proceedings of the 5th EPAC, Barcelona, vol. 3, pp. 2213-2215, 1996.
- [7] M. M. Gordon, "Calculation of isochronous fields for sector-focused cyclotrons", Part. Accel., vol. 13, pp. 67-84, 1983.